Optical properties of BaFe2-xCoxAs2

van Heumen, E.; Huang, Y.; de Jong, S.; Kuzmenko, A.B.; Golden, M.S.; van der Marel, D.

DOI
10.1209/0295-5075/90/37005

Publication date
2010

Document Version
Final published version

Published in
Europhysics Letters

Optical properties of $BaFe_{2-x}Co_xAs_2$

2010 EPL 90 37005

(http://iopscience.iop.org/0295-5075/90/3/37005)

A Letters Journal Exploring the Frontiers of Physics

May 2010

EPL, **90** (2010) 37005 www.epljournal.org
doi: 10.1209/0295-5075/90/37005

Optical properties of $BaFe_{2-x}Co_xAs_2$

E. van Heumen[1,2(a)], Y. Huang[2], S. de Jong[2], A. B. Kuzmenko[1], M. S. Golden[2] and D. van der Marel[1]

[1] *Département de Physique de la Matière Condensée, Université de Genève - quai Ernest-Ansermet 24, CH1211, Genève 4, Switzerland*
[2] *Van der Waals-Zeeman Institute, University of Amsterdam - NL-1018XE Amsterdam, The Netherlands, EU*

received 4 December 2009; accepted in final form 3 May 2010
published online 1 June 2010

PACS 74.25.Gz – Optical properties
PACS 74.25.-q – Properties of superconductors
PACS 74.70.Xa – Pnictides and chalcogenides

Abstract – We present detailed temperature-dependent optical data on $BaFe_{2-x}Co_xAs_2$ (BCFA), with $x = 0.14$, between 4 meV and 6.5 eV. We analyze our spectra to determine the main optical parameters and show that in this material the interband conductivity already starts at energies as low as 10 meV. We determine the superfluid density $\rho_s/(2\pi c)^2 = 2.2 \pm 0.5 \cdot 10^7\,\mathrm{cm}^{-2}$, which places optimally doped BFCA close to the Uemura line. Our experimental data shows clear signs of a superconducting gap with $2\Delta_1 = 6.2 \pm 0.8$ meV. In addition, from comparing the experimental spectra to model calculations we obtain indications for an additional band of strongly scattered carriers with a larger gap, $2\Delta_2 = 14 \pm 2$ meV.

Recently a new family of superconductors was discovered: the iron-pnictide superconductors [1]. Several studies indicate that these materials are much closer to conventional Fermi liquids with moderate interaction strengths [2–4], as compared to the strongly interacting cuprate superconductors. The parent iron pnictides are metallic with the states at the Fermi level deriving from the Fe orbitals [5] and, apart from an overall scaling factor of the bandwidth, appear to adhere to a conventional LDA framework [3]. In angle-resolved photoemission spectroscopy (ARPES) studies of K- and Co-doped $BaFe_2As_2$ (Ba122) momentum-independent superconducting gaps are observed on several Fermi surface sheets [6,7]. Optical experiments have been carried out on several members of the pnictide family. In the parent compounds a sizable Drude peak is present at high temperatures providing evidence for the metallic nature of the parent compounds. The transition into the orthorhombic spin ordered state is accompanied by a strong reduction of the carrier density and scattering rate [8] and an enhancement of the charge carrier mass [9], suggesting an interaction between the electrons and spin fluctuations. Experiments on superconducting LaFePO show that the experimentally determined plasma frequency is smaller by a factor of two to values obtained from bandstructure calculations [10], suggesting that the iron pnictides are in a moderately correlated regime. An analysis of the optical properties of $Ba_{0.55}K_{0.45}Fe_2As_2$, which has the highest critical temperature of the iron pnictide M-122 family, suggests that the charge carriers interact with a broad bosonic spectrum of spin fluctuations [11]. Studies of the effect of superconductivity on the optical properties are few. The observation of two gaps has been reported for $Ba_{0.6}K_{0.4}Fe_2As_2$ [12]. In this letter we present optical data on optimally doped $BaFe_{2-x}Co_xAs_2$ (BFCA) with a critical temperature T_c of 23 K. We observe the direct impact of superconductivity on the low-frequency optical spectrum and estimate the superconducting gap to be $2\Delta \approx 6.2 \pm 0.8$ meV. We extract the superfluid density $\rho_s/(2\pi c)^2 = 2.2 \pm 0.5 \cdot 10^7\,\mathrm{cm}^{-2}$ which places BFCA close to the Uemura line. We also test whether our results support the presence of a second gap.

Single crystals of BFCA were grown from self-flux and the results presented here are obtained on an $x = 0.14$ Co-doped sample. Co doping takes place in the Fe layers (see the crystal structure in fig. 1a). Our crystals exhibit a sharp bulk superconducting (SC) transition at $T_c = 23$ K as indicated by susceptibility and resistivity measurements on a crystal from the same batch (fig. 1b and c). The resistivity shows no sign of the anomalies associated with the structural and spin ordering transitions at higher temperatures. The reflectivity has been measured between 4 meV and 0.75 eV. Ellipsometric measurements were made in the range 0.75 eV to 6.5 eV. Experiments were performed

(a) E-mail: e.vanheumen@uva.nl

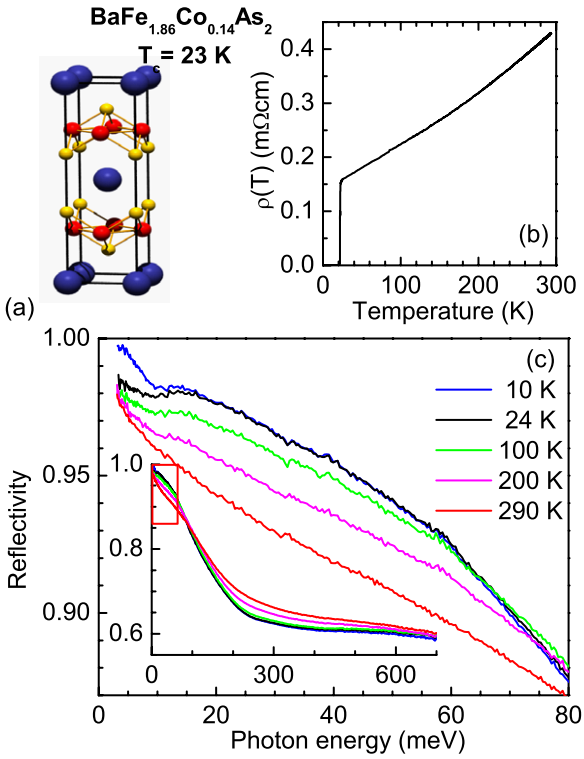

Fig. 1: (Colour on-line) (a) Unit cell of the tetragonal $BaFe_2As_2$ structure. Magnetic susceptibility measured with $H = 10$ Oe. (b) Temperature dependence of the resistivity. (c) Far-infrared reflectance for selected temperatures. Note the strong increase in reflectance below 10 meV for data taken at 10 K in the SC state.

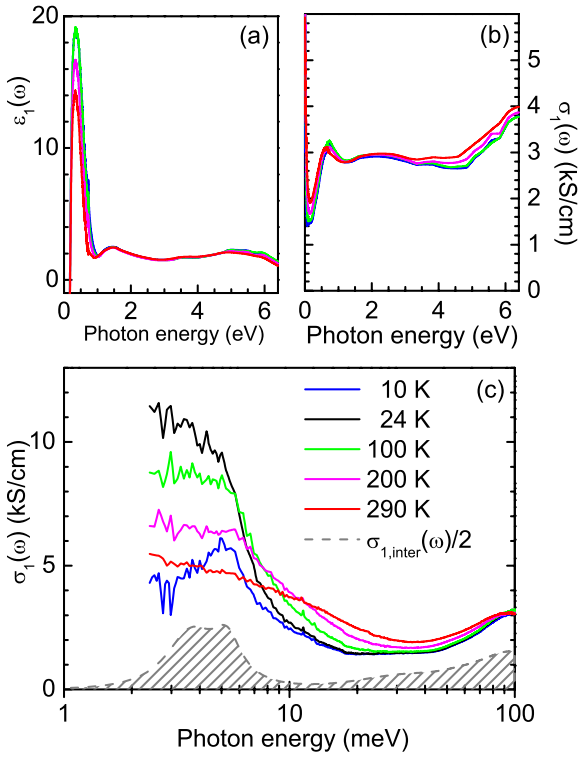

Fig. 2: (Colour on-line) (a) Dielectric function for selected temperatures (indicated in panel (c)). Above 750 meV the dielectric function is only weakly frequency dependent. (b) Optical conductivity at the same temperatures. (c) Optical conductivity on a logarithmic energy scale. The shaded area indicates the contribution to the conductivity from interband transitions at 24 K (divided by two for clarity of presentation).

between 10 K and 300 K, using stabilized, high-vacuum cryostats ($\leqslant 10^{-9}$ mbar in the MIR to UV range).

The reflectivity is shown in fig. 1c. It scales at room temperature as $R(\omega) \approx 1 - A\sqrt{\omega}$ for small frequencies, which is the Hagen-Rubens behavior expected for a metal. Below the critical temperature there is a clear impact of superconductivity on the reflectivity, pushing the reflectivity to unity below 5 meV. The reflectivity is shown on the entire measured range in the inset of fig. 1c. The ellipsometric data is presented in fig. 2a and b. The optical conductivity (fig. 2b) has maxima around 2.5 and 3.9 eV, which we interpret as interband transitions (fig. 2b). The low-energy tail of a third transition can be seen, which has its maximum outside our experimental range. The observed transitions correspond reasonably well with those observed in DMFT calculations on LaOFeAs [13]. The peak around 2 eV is attributed to transitions from Fe 3d to As 4p states while a larger peak at higher energy (4–6 eV) is related to transitions within the Fe d shell.

We extract the complex optical conductivity from the measured reflectivity and ellipsometric data using a Kramers-Kronig consistent variational routine [14]. The dielectric function, $\varepsilon_1(\omega)$, and optical conductivity, $\sigma_1(\omega)$, are shown in fig. 2a and b. The low-frequency conductivity is shown in fig. 2c. It is composed of a Drude-like peak that narrows with decreasing temperature and several low-energy absorptions, which are more clearly visible at low temperatures. The dashed gray area in fig. 2c represents the interband contribution obtained from a Drude-Lorentz fit at 24 K (divided by two for clarity). The parameters of the model are presented in table 1. We observe an absorption around 10 meV. From LDA band calculations of the optical conductivity (see [15]) we know that the onset of interband transitions occurs at very low energy in these compounds due to the fact that several bands cross close to the Fermi energy. The interpretation of the observed onset of optical conductivity at 10 meV as interband transitions is therefore plausible. We also observe a sharp onset of interband transitions around 60 meV, which is reflected by a downward kink in the reflectivity at lower temperatures, followed by a distinct mid-infrared peak at 0.62 eV. Having determined the main optical features we now turn our attention to the quantities that characterize the superconducting state. An important quantity measuring the robustness of the SC state is the superfluid density ρ_s. The presence of a superfluid density gives rise to a zero-frequency condensate peak in the optical conductivity with an area $\rho_s = \omega_{p,s}^2$. Since the total spectral

Table 1: Oscillator parameters of the normal-state ($T = 24\,\mathrm{K}$) Drude-Lorentz modeling of the optical conductivity. ω_p and γ in the case of the Drude term correspond to the plasma frequency and scattering rate, respectively. The parameters ω_o, A and γ are the centre frequency, oscillator strength and damping coefficient of a Lorentzian oscillator. The contribution of high-energy interband transitions is given by $\epsilon_\infty = 2.84$.

Drude terms (meV)	
$\hbar\omega_p$	$\hbar\gamma$
750	6
890	46

Phonon (meV)		
$\hbar\omega_o$	A	$\hbar\gamma$
32	30	0.7

Interband transitions (eV)		
$\hbar\omega_o$	A	$\hbar\gamma$
0.006	0.43	0.005
0.01	0.38	0.005
0.13	1.27	0.24
0.32	0.9	0.3
0.64	3.7	0.82
2.5	10	5.3
3.9	2.5	2.2
6.6	7.8	3.2

weight above and below the critical temperature has to remain constant, one can measure the superfluid density by analyzing the reduction of finite frequency spectral weight when the material becomes superconducting [16]. Using this Ferrell-Glover-Tinkham sum rule we determine $\rho_s/(2\pi c)^2 = 2.2 \pm 0.5 \cdot 10^7\,\mathrm{cm}^{-2}$ (corresponding to a penetration depth of 340 nm for $T = 10\,\mathrm{K}$), in agreement with the result obtained in ref. [17]. The same analysis shows that the superconductivity-induced transfer of spectral weight is recovered around 40 meV. A second method to determine ρ_s follows by making use of the Kramers-Kronig (KK) relations [18]: if a zero-frequency δ-peak of strength $\omega_{p,s}^2$ is present in $\sigma_1(\omega)$, applying the KK relations will lead to $\varepsilon_1(\omega) \propto -\omega_{p,s}^2/\omega^2$. Therefore, the fact that the zero-frequency extrapolation of $-\omega^2\varepsilon_1(\omega)$ is non-zero is a direct consequence of the presence of a superfluid condensate. We show $-\omega^2\varepsilon_1(\omega)$ in fig. 3. We see that the extrapolation to zero of the experimental curve at 10 K matches reasonably well with the value estimated from the spectral weight analysis. Estimates of the penetration depth $\lambda(0) \approx 208\,\mathrm{nm}$ on optimally doped BFCA crystals were reported in ref. [19] based on measurements of H_{c1}. To compare this with our results one has to take into account the fact that our measurement is performed at 10 K. From the temperature dependence of $\Delta\lambda(T)$ also reported in [19] we obtain $\lambda(10\,\mathrm{K}) \approx 350\,\mathrm{nm}$. This value is close to the Uemura relation $\rho_s \propto T_c$ [20] putting T_c an order of magnitude below the Fermi temperature $\approx dk_B^{-1}(\hbar/2e)^2\rho_s = 440\,\mathrm{K}$. For K-doped Ba122 with $T_c = 36\,\mathrm{K}$ the superfluid density is an order of magnitude larger [21].

The second quantity characterizing the superconducting state is the superconducting gap. At zero temperature

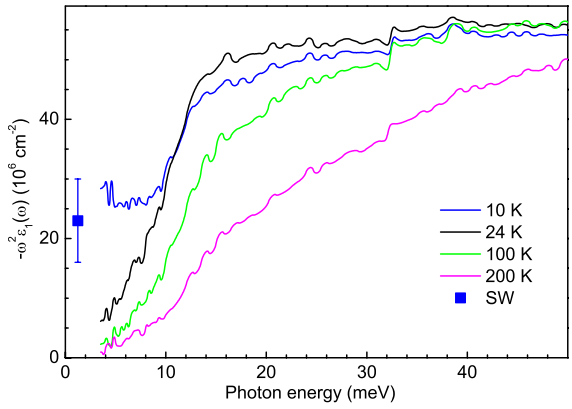

Fig. 3: (Colour on-line) $-\omega^2\varepsilon_1(\omega)$ for several temperatures. The extrapolation to zero frequency gives an estimate of the superfluid density. All normal-state data extrapolates to zero at zero frequency, while the $T = 10\,\mathrm{K}$ data extrapolates to a finite value. The blue square indicates ρ_s estimated from a spectral weight analysis.

the gap can be determined from the onset of absorption in the optical conductivity, but temperature broadening and the uncertainties related to the determination of the deviation of the reflectivity from unity make a reliable determination of the gap size in this manner difficult to realize. A method to determine the SC gap directly from experimental data was proposed by Marsiglio *et al.* [22] based on the KK relations. They showed that BCS theory predicts a cusp-like minimum in $-\omega^2\varepsilon_1(\omega)$ at 2Δ for weak impurity scattering. Figure 3 shows such a minimum around $2\Delta \approx 6\,\mathrm{meV}$, but the experimental noise makes an accurate determination of the gap size impossible. To test whether our optical data supports the presence of one or more superconducting gaps, we use an analysis based on a method put forward by Zimmermann *et al.* [23]. These authors derive expressions for the optical conductivity of a BCS superconductor with arbitrary impurity scattering, implemented in a fast computational routine that allows for direct least-square optimization of the model parameters using experimental data (employing the standard Fresnel equations to obtain the reflectivity). To calculate the optical conductivity in this framework requires 4 input parameters: the reduced temperature $t = T/T_c$, gap value Δ, plasma frequency ω_p and impurity scattering rate $\gamma = 1/\tau$. In these multiband systems we expect to have more than one band contributing to the conductivity (also evidenced by the presence of two Drude terms, see table 1), we assume that the conductivity can be described by the superposition of two independent channels: $\sigma(\omega, T) = \sigma(\omega, \Delta_1, \gamma_1, \omega_{p,1}, T) + \sigma(\omega, \Delta_2, \gamma_2, \omega_{p,2}, T)$. First we optimize the parameters of a standard Drude-Lorentz model at 24 K. We assume that at lower temperatures the occurrence of superconductivity only affects the Drude terms of the model. In the next step we take the estimate of the gap value, $\Delta_1 = 3\,\mathrm{meV}$, obtained from $-\omega^2\varepsilon_1$ for the small gap and a larger one, $\Delta_2 = 7\,\mathrm{meV}$, which has been observed in ARPES [7] and STS experiments [24]

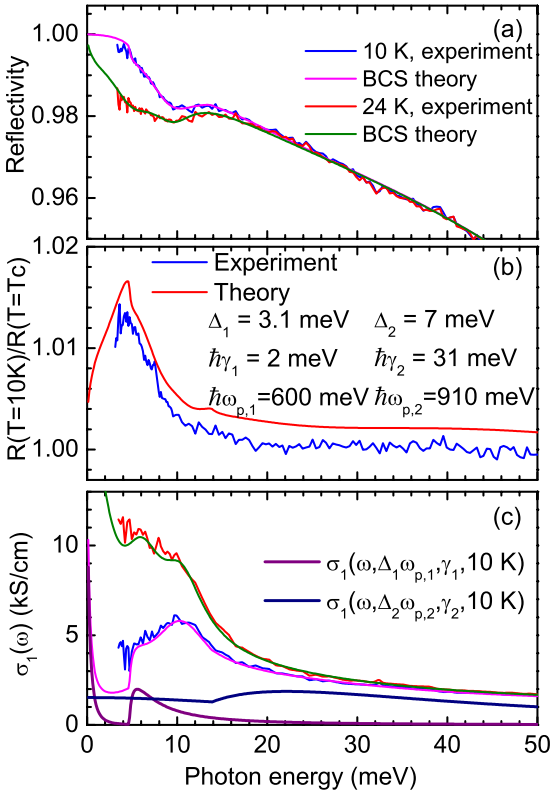

Fig. 4: (Colour on-line) (a) Low-energy experimental reflectivity (blue) and reflectivity obtained from the BCS simulation (violet) at 10 K. Also shown are the reflectivity (red) and Drude-Lorentz model result (green) at T_c. (b) Ratio of 10 K reflectivity to the one at T_c (24 K) for the experimental data (blue) and simulation (offset for clarity by multiplication with a factor of 1.002, in red). (c) Comparison of the 10 K optical conductivity determined from experiment (blue) and simulation (violet) and the 24 K data (red) and Drude-Lorentz model (green). Note the low-frequency upturn in the simulation which arises from finite temperature broadening. We also show the two contributions to the conductivity from the BCS calculation.

on compounds with a similar Co content. We then use a least-squares optimization routine to optimize the parameters of the model, keeping the parameters describing the interband contributions fixed. From this process we find $\Delta_1 = 3.1\,\mathrm{meV}$, $\hbar\omega_{p,1} = 0.6\,\mathrm{eV}$ and $\hbar\gamma_1 = 2\,\mathrm{meV}$ for the first term and $\Delta_2 = 7\,\mathrm{meV}$, $\hbar\omega_{p,2} = 0.9\,\mathrm{eV}$, and $\hbar\gamma_2 = 31\,\mathrm{meV}$ for the second term. Figure 4a shows the reflectivity data at 10 K and T_c. Also shown are fits to the data obtained from BCS theory at 10 K and the Drude-Lorentz model at 24 K. The gap-induced features are more clearly seen in the ratio of the reflectivity at 10 K to that at T_c (fig. 4b). The simulated curve has been offset for clarity. In fig. 4c we compare the optical conductivity with the BCS conductivity at 10 K and the Drude-Lorentz model at 24 K. Note the substantial conductivity predicted by the simulation in the region below $2\Delta_1$, which arises from thermal excitations of unpaired electrons. By shifting the reflectivity up and down by 0.5% and repeating the analysis we obtain error bars on the determined values: $\Delta_1 = 3.1 \pm 0.4\,\mathrm{meV}$ and $\Delta_2 = 7 \pm 1\,\mathrm{meV}$. In fig. 4c we also show the decomposition of the BCS conductivity in the individual conductivity channels. We see that the small-gap contribution (purple) gives rise to a pronounced structure in the conductivity, but the contribution associated with the larger gap (navy blue) is rather featureless due to the large scattering rate. The assignment to the smaller gap at $2\Delta_1 = 6.2\,\mathrm{meV}$ is unambiguously supported by the optical spectra. Our data is also consistent with the existence of a larger gap at $2\Delta_2 = 14\,\mathrm{meV}$, but the interpretation of the corresponding spectral features is probably not unique. STM experiments on samples from the same batch show an average superconducting gap of $2\Delta = 14\,\mathrm{meV}$ [24]. The large gap obtained by ARPES experiments is found on a barrel around the Γ-point, which is connected by a nesting vector $Q = (\pi, \pi)$ (in the folded zone) to a barrel around X, exhibiting a smaller gap [7]. In these experiments there is only one hole pocket around the Γ-point while there are two electron pockets around the X-point, which gives rise to a relative enhancement of the scattering rate on the hole pocket. This is in line with our observation of a larger scattering rate associated with the large gap. Interestingly, the absence of a clear optical signature of a second, larger gap was also the case in data on MgB_2 [25], where overwhelming evidence for the existence of two distinct gaps was found by other spectroscopies.

In conclusion, we have presented a detailed analysis of the optical spectra of BFCA. The optical spectrum is characterized by a Drude-like peak and several interband transitions. We find that the low-frequency conductivity already has a substantial contribution from interband transitions as may be expected in a multiband system. The superfluid density is much smaller compared to its hole doped cousin $Ba_{1-x}K_xFe_2As_2$. We directly observe a small superconducting gap with $2\Delta_1 = 6.2\,\mathrm{meV}$. However, a single gap cannot explain all low-energy features of the optical conductivity spectra. These spectra can be fully explained if we assume the presence of an additional band of strongly scattered carriers with a larger gap, $2\Delta_2 = 14\,\mathrm{meV}$.

* * *

We would like to thank H. Luigjes, R. Huisman and A. de Visser for the resistivity measurement. This work is supported by the Swiss National Science Foundation through Grant No. 200020-113293 and the National Center of Competence in Research (NCCR) "Materials with Novel Electronic Properties", MaNEP, and is, in addition, part of the research programme of the Foundation for Fundamental Research on Matter (FOM), which is financially supported by the Netherlands Organisation for Scientific Research (NWO).

Additional remark: After submission we became aware of a paper by Kim *et al.* [26] where evidence is found for two

or three superconducting gaps. The smallest gap reported there has $2\Delta \approx 3.7\,\mathrm{meV}$, consistent with our result.

REFERENCES

[1] Kamihara Y., Watanabe T., Hirano M. and Hosono H., *J. Am. Chem. Soc.*, **130** (2008) 3296.

[2] Mazin I. I., Singh D. J., Johannes M. D. and Du M. H., *Phys. Rev. Lett.*, **101** (2008) 057003.

[3] Lu D., Yi M., Mo S.-K., Erickson A., Analytis J., Chu J.-H., Singh D., Hussain Z., Geballe T., Fisher I. and Shen Z.-X., *Nature*, **455** (2008) 81.

[4] Chubukov A. V., Efremov D. V. and Eremin I., *Phys. Rev. B*, **78** (2008) 134512.

[5] de Jong S., Huang Y., Huisman R., Massee F., Thirupathaiah S., Gorgoi M., Schaefers F., Follath R., Goedkoop J. B. and Golden M. S., *Phys. Rev. B*, **79** (2009) 115125.

[6] Evtushinsky D. V., Inosov D. S., Zabolotnyy V. B., Koitzsch A., Knupfer M., Büchner B., Viazovska M. S., Sun G. L., Hinkov V., Boris A. V., Lin C. T., Keimer B., Varykhalov A., Kordyuk A. A. and Borisenko S. V., *Phys. Rev. B*, **79** (2009) 054517.

[7] Terashima K., Sekiba Y., Bowen J. H., Nakayama K., Kawahara T., Sato T., Richard P., Xu Y.-M., Li L. J., Cao G. H., Xu Z.-A., Ding H. and Takahashi T., *Proc. Natl. Acad. Sci. U.S.A.*, **106** (2009) 7330.

[8] Hu W. Z., Dong J., Li G., Li Z., Zheng P., Chen G. F., Luo J. L. and Wang N. L., *Phys. Rev. Lett.*, **101** (2008) 257005.

[9] Wu D., Barišić N., Drichko N., Kaiser S., Faridian A., Dressel M., Jiang S., Ren Z., Li L. J., Cao G. H., Xu Z. A., Jeevan H. S. and Gegenwart P., *Phys. Rev. B*, **79** (2009) 1.

[10] Qazilbash M. M., Hamlin J. J., Baumbach R. E., Zhang L., Singh D. J., Maple M. B. and Basov D. N., *Nat. Phys.*, **5** (2009) 647.

[11] Yang J., Hüvonen D., Nagel U., om T. R. o., Ni N., Canfield P. C., Bud'ko S. L., Carbotte J. P. and Timusk T., *Phys. Rev. Lett.*, **102** (2009) 187003.

[12] Li G., Hu W. Z., Dong J., Li Z., Zheng P., Chen G. F., Luo J. L. and Wang N. L., *Phys. Rev. Lett.*, **101** (2008) 107004.

[13] Haule K., Shim J. H. and Kotliar G., *Phys. Rev. Lett.*, **100** (2008) 1.

[14] Kuzmenko A. B., *Rev. Sci. Instrum.*, **76** (2005) 083108.

[15] Hancock J. N., Mirzaei S. I., Gillett J., Sebastian S. E., Teyssier J., Viennois R., Giannini E. and van der Marel D., arXiv:1004.0111v1 (2010).

[16] Tinkham M. and Ferrell R., *Phys. Rev. Lett.*, **2** (1959) 331.

[17] Wu D., Barišić N., Drichko N., Kallina P., Faridian A., Gorshunov B., Dressel M., Li L. J., Lin X., Cao G. H. and Xu Z. A., to be published in *Physica C* (2009).

[18] Basov D. N., Liang R., Bonn D. A., Hardy W. N., Dabrowski B., Quijada M., Tanner D. B., Rice J. P., Ginsberg D. M. and Timusk T., *Phys. Rev. Lett.*, **74** (1995) 598.

[19] Gordon R. T., Ni N., Martin C., Tanatar M. A., Vannette M. D., Kim H., Samolyuk G. D., Schmalian J., Nandi S., Kreyssig A., Goldman A. I., Yan J. Q., Bud'ko S. L., Canfield P. C. and Prozorov R., *Phys. Rev. Lett.*, **102** (2009) 127004.

[20] Uemura Y. J., Le L. P., Luke G. M., Sternlieb B. J., Wu W. D., Brewer J. H., Riseman T. M., Seaman C. L., Maple M. B., Ishikawa M., Hinks D. G., Jorgensen J. D., Saito G. and Yamochi H., *Phys. Rev. Lett.*, **66** (1991) 2665.

[21] Ren C., Wang Z., Luo H., Yang H. and Shan L., *Phys. Rev. Lett.*, **101** (2008) 257006.

[22] Marsiglio F., Carbotte J., Puchkov A. and Timusk T., *Phys. Rev. B*, **53** (1996) 9433.

[23] Zimmermann W., Brandt E., Bauer M., Seider E. and Genzel L., *Physica C*, **183** (1991) 99.

[24] Massee F., Huang Y., Huisman R., de Jong S., Goedkoop J. B. and Golden M. S., *Phys. Rev. B*, **79** (2009) 220517.

[25] Kuzmenko A., *Physica C*, **456** (2007) 63.

[26] Kim K. W. *et al.*, arXiv:0912.0140v1 [cond-mat.supr-con].